Astron. Astrophys. 320, 333–341 (1997)

ASTRONOMY AND ASTROPHYSICS

# UV and soft X-ray lines from Fe XVI observed in solar and stellar spectra

**M. Cornille**[1], **J. Dubau**[1], **H.E. Mason**[2], **C. Blancard**[3], **and W.A. Brown**[4]

[1] Observatoire de Paris, UPR 176 CNRS, DARC F-92195 Meudon-Cedex, France
[2] Department of Applied Mathematics and Theoretical Physics, Silver Street, CAMBRIDGE CB3 9EW, UK
[3] Centre d'Etudes de Limeil-Valenton, F-94195 Villeneuve Saint Georges Cedex, France
[4] Lockheed Palo Alto Research Laboratory, Palo Alto California 94304, USA

Received 27 June 1996 / Accepted 12 September 1996

**Abstract.** The ion Fe XVI is abundant in solar active regions and flares. Strong spectral lines from this ion have been observed over a wide wavelength range. The transitions 3s - 3p and 3p - 3d fall between 250 and 365Å and lines from transitions between n=3 to n=4, n=3 to n=5 fall between 30 and 80 Å. In this paper, we present distorted wave results for the electron scattering collision strengths from the ground level to all the other levels and discuss previous calculations. We compare our theoretical intensity ratios with solar observations and show that the strongest spectral lines in the X-ray wavelength range do not correspond to the dipole transitions, 3s - 4p, 3s - 5p, as might be expected. We comment on the approximations which have been generally used in synthetic spectrum programs to simulate the Fe XVI spectral line intensities and the consequences for analyses of solar and stellar spectra.

**Key words:** atomic data – Sun: corona – Sun: UV – stars: coronae – ultraviolet: stars

## 1. Introduction

Accurate electron scattering calculations are now available for many of the ions which are abundant in the solar corona and transition region. These were reviewed at an atomic data assessment workshop held in Abingdon in 1992 (Lang, 1994). In the 1970's, new calculations were prompted by the Skylab UV observations. Recent interest has revived in the UV wavelength range with the succesful flights of the SERTS (Solar EUV Rocket Telescope and Spectrometer) (Neupert et al, 1992). In addition a major satellite mission, the Solar Heliospheric Observatory (SOHO) was launched in December 1995. This carries several UV spectroscopic instruments, including the Coronal Diagnostic Spectrometer (CDS) (160-800Å) (Harrison and Sawyer, 1992) and the Solar Ultraviolet Measurement of Emitted Radiation (SUMER) instrument (Lemaire *et al*, 1992). An extensive review of observations and spectroscopic diagnostics in the VUV wavelength range for both solar and stellar plasmas is given by Mason and Monsignori Fossi (1994). The emphasis in the past decade has been on solar flare spectra. This interest was stimulated by the success of projects such as the Solar Maximum Mission, SOLEX, SOLFLEX, HINOTORI and more recently YOHKOH. These instruments obtained high resolution spectra in the X-ray wavelength regions, below 25 Å. In this paper, we concentrate on the wavelength region beyond this, up to 100Å, which was observed with the grazing incidence spectrograph (XSST) flown on a rocket (Acton *et al*, 1985). In particular, we are interested by the strong Fe XVI lines which are prominent in these spectra. We note that the spectral lines corresponding to transitions between 3p - 4s, 3p - 4d and 3p - 4f are as strong as the spectral lines corresponding to 3s - 4p transitions. A similar phenomena is seen for the spectral lines for n=3 to n=5 transitions. To investigate the observed line intensities, we have carried out distorted wave (DW) calculations of the electron excitation rates using the DISTWAV program developed at University College London (UCL) and a new program - NELMA - (Non-exchange Limeil Meudon Approximation) developed by Blancard and Dubau. We compare the accuracy of this approach with other published electron scattering calculations for Fe XVI. We compute the theoretical intensities for the Fe XVI X-ray lines under solar conditions. We also comment on the important implications of our results for analyses of stellar spectra. Initial results for Fe XVI were presented by Cornille *et al* (1993).

## 2. Atomic structure calculations

We have obtained energy levels, oscillator strengths and radiative transition probabilities for Fe XVI using the Superstructure (SSTRUCT) program developed at UCL (Eissner *et al*, 1974). This program uses a scaled Thomas Fermi potential for the one electron orbitals. We have used the scaling parameters $\lambda_s = 1.1257, \lambda_p = 1.0363, \lambda_d = 1.0010, \lambda_f = 0.9713$ obtained

*Send offprint requests to*: M. Cornille

**Table 1.** Energy levels

| i | Config-uration | Level | Theoretical Rydbergs | Energy $cm^{-1}$ | Reader& Sugar (1975) $cm^{-1}$ |
|---|---|---|---|---|---|
| 1 | 3s | $^2S_{0.5}$ | 0 | 0 | 0 |
| 2 | 3p | $^2P_{0.5}$ | 2.530 | 277644 | 277160 |
| 3 | | $^2P_{1.5}$ | 2.716 | 298071 | 298140 |
| 4 | 3d | $^2D_{1.5}$ | 6.179 | 678044 | 675470 |
| 5 | | $^2D_{2.5}$ | 6.209 | 681357 | 678420 |
| 6 | 4s | $^2S_{0.5}$ | 17.017 | 1867439 | 1867530 |
| 7 | 4p | $^2P_{0.5}$ | 18.021 | 1977565 | 1978040 |
| 8 | | $^2P_{1.5}$ | 18.093 | 1985477 | 1986100 |
| 9 | 4d | $^2D_{1.5}$ | 19.364 | 2124926 | 2124080 |
| 10 | | $^2D_{2.5}$ | 19.377 | 2126356 | 2125360 |
| 11 | 4f | $^2F_{2.5}$ | 19.914 | 2185355 | 2184610 |
| 12 | | $^2F_{3.5}$ | 19.919 | 2185859 | 2185170 |
| 13 | 5s | $^2S_{0.5}$ | 24.266 | 2662852 | 2662000 |
| 14 | 5p | $^2P_{0.5}$ | 24.760 | 2717144 | 2717170 |
| 15 | | $^2P_{1.5}$ | 24.796 | 2721033 | 2721160 |
| 16 | 5d | $^2D_{1.5}$ | 25.409 | 2788310 | 2788020 |
| 17 | | $^2D_{2.5}$ | 25.416 | 2789043 | 2788610 |
| 18 | 5f | $^2F_{2.5}$ | 25.686 | 2818761 | 2818590 |
| 19 | | $^2F_{3.5}$ | 25.689 | 2819020 | 2818920 |

by minimising all the term energies. Spin-orbit and relativistic corrections are treated as a perturbation to the non-relativistic Hamiltonian and the results are given in intermediate coupling. In Table 1, we give the theoretical energy values and find excellent agreement with the observed energy values (Reader and Sugar, 1975). In Table 2, we give the dipole oscillator strengths and the radiative transition probabilities.

## 3. Electron scattering calculations

The electron scattering calculation for the low partial wave values of the incoming electron was carried out using the distorted wave approximation with a program developed at UCL (DISTWAV) (Eissner, 1972, Eissner and Seaton, 1972). Collision strengths are obtained in pair coupling using the program JAJOM (Saraph, 1970, 1972, 1978), including term coupling coefficients from SSTRUCT. This has been used extensively to calculate excitation rates for ions which are abundant in the solar transition region and corona. The agreement between the distorted wave results and the more sophisticated close-coupling results is found to be excellent for highly ionised systems, such as coronal ions (Burgess *et al*, 1989, 1991). The program DISTWAV is used for low partial wave values ( $l \leq l_a - 1$). For the dipole transitions, the Coulomb Bethe approximation (Burgess and Shoerey, 1974) is used for higher partial wave contributions $l_a \leq l \leq 200$ to the dipole transitons (where $l_a$ = 20 for 26 and 50 Ryd and $l_a$ = 25 for 100 and 200 Ryd). The convergence of the distorted wave and Coulomb Bethe approx-

**Table 2.** Radiative data

| Transition j i | A(j,i) $s^{-1}$ | $\omega_i f_{ij}$ | $\lambda_{ij}$ Theoretical |
|---|---|---|---|
| 2 1 | 6.406E+09 | 2.942E-1 | 360.17 |
| 3 1 | 7.969E+09 | 5.379E-1 | 335.49 |
| 4 2 | 1.572E+10 | 5.880E-1 | 249.75 |
| 4 3 | 2.699E+09 | 1.121E-1 | 263.18 |
| 5 3 | 1.665E+10 | 1.019E 0 | 260.90 |
| 6 2 | 1.047E+11 | 1.243E-1 | 62.90 |
| 6 3 | 2.191E+11 | 2.667E-1 | 63.72 |
| 7 1 | 1.984E+11 | 1.521E-1 | 50.57 |
| 7 4 | 7.635E+10 | 1.365E-1 | 76.95 |
| 7 6 | 1.467E+09 | 3.627E-1 | 908.05 |
| 8 1 | 1.893E+11 | 2.880E-1 | 50.37 |
| 8 4 | 7.313E+09 | 2.566E 0 | 76.49 |
| 8 5 | 6.652E+10 | 2.346E-1 | 76.68 |
| 8 6 | 1.809E+09 | 7.784E-1 | 847.18 |
| 9 2 | 3.410E+11 | 5.993E-1 | 54.13 |
| 9 3 | 6.977E+10 | 1.254E-1 | 54.74 |
| 9 7 | 3.394E+09 | 9.373E-1 | 678.61 |
| 10 3 | 4.166E+11 | 1.121E 0 | 54.70 |
| 10 8 | 3.564E+09 | 1.615E 0 | 709.83 |
| 11 4 | 9.324E+11 | 3.692E 0 | 66.34 |
| 11 5 | 6.645E+10 | 2.643E-1 | 66.49 |
| 12 5 | 9.974E+11 | 5.285E 0 | 66.47 |
| 13 2 | 4.529E+10 | 2.387E 0 | 41.93 |
| 13 3 | 9.999E+10 | 5.361E 0 | 42.29 |
| 13 7 | 3.315E+10 | 2.117E-1 | 145.92 |
| 13 8 | 6.939E+10 | 4.534E-1 | 147.63 |
| 14 1 | 1.148E+11 | 4.664E-1 | 36.80 |
| 14 4 | 2.799E+10 | 2.019E 0 | 49.04 |
| 14 6 | 3.888E+10 | 1.615E-1 | 117.69 |
| 14 9 | 3.538E+10 | 3.025E-1 | 168.86 |
| 15 1 | 1.129E+11 | 9.145E 0 | 36.75 |
| 15 4 | 2.702E+09 | 3.883E-3 | 48.95 |
| 15 5 | 2.507E+10 | 3.614E 0 | 49.03 |
| 15 6 | 3.717E+10 | 3.060E-1 | 117.15 |
| 15 9 | 3.440E+09 | 5.806E 0 | 167.76 |
| 15 10 | 3.130E+10 | 5.309E-1 | 168.16 |
| 16 2 | 1.959E+11 | 1.863E-1 | 39.83 |
| 16 3 | 4.085E+10 | 3.950E 0 | 40.16 |
| 16 7 | 5.514E+10 | 5.031E-1 | 123.34 |
| 16 8 | 1.164E+10 | 1.083E-1 | 124.56 |
| 16 11 | 6.388E+09 | 1.054E-1 | 165.85 |
| 16 14 | 1.056E+09 | 1.250E 0 | 1405.17 |
| 17 3 | 2.455E+11 | 3.558E-1 | 40.15 |
| 17 8 | 6.941E+10 | 9.669E-1 | 124.45 |
| 17 12 | 6.071E+09 | 1.501E-1 | 165.79 |
| 17 15 | 1.102E+09 | 2.143E 0 | 1470.37 |
| 18 4 | 3.437E+11 | 6.747E-1 | 46.71 |
| 18 5 | 2.448E+10 | 4.821E 0 | 46.79 |
| 18 9 | 1.535E+11 | 2.869E 0 | 144.13 |
| 18 10 | 1.099E+10 | 2.062E-1 | 144.42 |
| 19 5 | 3.684E+11 | 9.668E-1 | 46.78 |
| 19 10 | 1.648E+11 | 4.121E 0 | 144.37 |

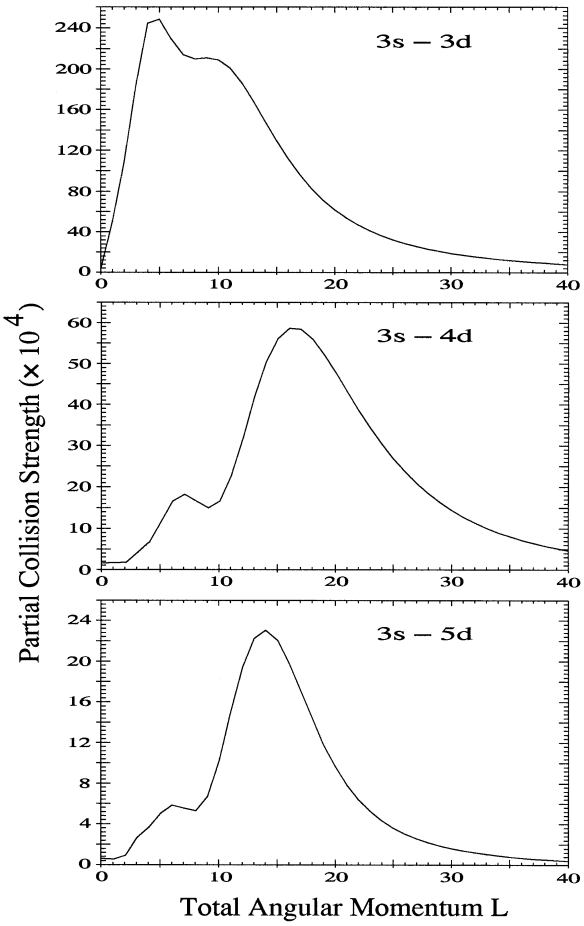


**Fig. 1.** Partial collision strengths : 3s - nd at 200 Ryd.

imations was checked. For the high incident energies - 100 Ryd. and 200 Ryd. calculations, there is a significant contribution to the quadrupole transitions (3s - 3d, 4d, 5d) beyond $l_a$. This is calculated using the program NELMA (Cornille *et al*, 1994). The program NELMA is a new code, which describes the target by a multi-configuration expansion and calculates the collision strengths in LS and intermediate coupling scheme using a distorted wave approximation without exchange. In this program the unitarity of the transition matrix T is omitted. In Fig. 1 we show the partial collision strengths for these transitions. The slow convergence for high partial wave values is evident. Exchange is only important for the small partial wave values and the convergence of the DISTWAV and NELMA results have been thoroughly checked. It was found that the contribution of exchange to the 3s - nd transitions decreases with increasing energy of the incoming electron.

In Fig. 2, we give a comparison of the 3s - 4l transitions (3s-4d is given in Fig. 1).

In Tables 3-6, we give the values for the collision strengths obtained for Fe XVI at energies of the incoming electron relative to the ground configuration of 26, 50, 100 and 200 Ryd.

We see from Tables 3-6 that the electron collision strengths for the dipole transition 3s - 3p are greater than those for 3s

**Table 3.** Collision strengths

| Transition i j | Ω 26 Ryd | 50 Ryd | 100 Ryd | 200 Ryd |
|---|---|---|---|---|
| 1 2 | 1.615 | 1.848 | 2.132 | 2.401 |
| 1 3 | 3.230 | 3.697 | 4.268 | 4.809 |
| 1 4 | 0.133 | 0.132 | 0.139 | 0.137 |
| 1 5 | 0.200 | 0.200 | 0.209 | 0.206 |
| 1 6 | 0.0957 | 0.106 | 0.112 | 0.115 |
| 1 7 | 0.0073 | 0.0141 | 0.0273 | 0.0452 |
| 1 8 | 0.0141 | 0.0264 | 0.0508 | 0.0843 |
| 1 9 | 0.0188 | 0.0236 | 0.0294 | 0.0328 |
| 1 10 | 0.0281 | 0.0353 | 0.0443 | 0.0496 |
| 1 11 | 0.0358 | 0.0365 | 0.0380 | 0.0387 |
| 1 12 | 0.0477 | 0.0487 | 0.0508 | 0.0518 |
| 1 13 | 0.0148 | 0.0187 | 0.0208 | 0.0217 |
| 1 14 | 0.00193 | 0.00319 | 0.00609 | 0.0100 |
| 1 15 | 0.00406 | 0.00641 | 0.0120 | 0.0196 |
| 1 16 | 0.00617 | 0.00704 | 0.00866 | 0.00978 |
| 1 17 | 0.00929 | 0.01059 | 0.0131 | 0.0148 |
| 1 18 | 0.00794 | 0.00694 | 0.00684 | 0.00708 |
| 1 19 | 0.0106 | 0.00927 | 0.00914 | 0.00947 |
| 2 3 | 0.178 | 0.173 | 0.159 | 0.159 |
| 2 4 | 2.262 | 2.628 | 3.082 | 3.474 |
| 2 5 | 0.0359 | 0.0311 | 0.0306 | 0.0401 |
| 2 6 | 0.0140 | 0.0231 | 0.0386 | 0.0580 |
| 2 7 | 0.107 | 0.118 | 0.123 | 0.124 |
| 2 8 | 0.0174 | 0.0185 | 0.0202 | 0.170 |
| 2 9 | 0.0425 | 0.0812 | 0.144 | 0.213 |
| 2 10 | 0.0153 | 0.0130 | 0.0121 | 0.0118 |
| 2 11 | 0.125 | 0.160 | 0.191 | 0.181 |
| 2 12 | 0.0219 | 0.0151 | 0.0142 | 0.0153 |
| 2 13 | 0.00257 | 0.00345 | 0.00550 | 0.00805 |
| 2 14 | 0.0168 | 0.0205 | 0.0220 | 0.0226 |
| 2 15 | 0.00525 | 0.00455 | 0.00475 | 0.00470 |
| 2 16 | 0.0114 | 0.0212 | 0.0370 | 0.0543 |
| 2 17 | 0.00612 | 0.00412 | 0.0314 | 0.0337 |
| 2 18 | 0.0214 | 0.0262 | 0.00345 | 0.00345 |
| 2 19 | 0.00778 | 0.00385 | 0.00283 | 0.00292 |
| 3 4 | 0.495 | 0.563 | 0.654 | 0.744 |
| 3 5 | 4.100 | 4.758 | 5.579 | 6.299 |
| 3 6 | 0.0278 | 0.0485 | 0.0828 | 0.126 |
| 3 7 | 0.0174 | 0.0192 | 0.0214 | 0.0184 |
| 3 8 | 0.240 | 0.262 | 0.274 | 0.273 |
| 3 9 | 0.0280 | 0.0338 | 0.0463 | 0.0606 |
| 3 10 | 0.0960 | 0.169 | 0.288 | 0.418 |
| 3 11 | 0.0643 | 0.0661 | 0.0739 | 0.0726 |
| 3 12 | 0.232 | 0.289 | 0.342 | 0.326 |
| 3 13 | 0.00465 | 0.00635 | 0.0108 | 0.0167 |
| 3 14 | 0.00482 | 0.00432 | 0.00467 | 0.00475 |
| 3 15 | 0.0423 | 0.0491 | 0.0525 | 0.0535 |
| 3 16 | 0.00952 | 0.00920 | 0.0117 | 0.0154 |
| 3 17 | 0.0256 | 0.0420 | 0.0708 | 0.104 |
| 3 18 | 0.0160 | 0.0123 | 0.0124 | 0.0133 |
| 3 19 | 0.0412 | 0.0470 | 0.0553 | 0.0596 |

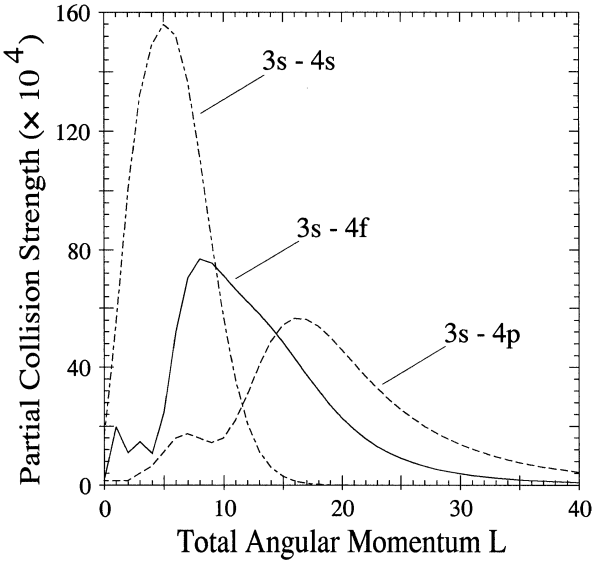


**Fig. 2.** Partial collision strengths : 3s - 4l at 200 Ryd. (full line is 3s - 4f, dashed line is 3s - 4p, dash-dot line is 3s - 4s)

- 3d. However, the electron collision strengths for the dipole transitions 3s - 4p are not greater than those for 3s - 4s, 3s - 4d or 3s - 4f at low energies. The same is true for the corresponding n=3 to n=5 transitions. A similar phenomena was found for transitions n=2 to n=3 in the Lithium like ions (McWhirter, 1994) and in the Beryllium like ions Fe XXIII and Ca XVII (Bhatia and Mason 1981, 1983). It was attributed by Bely *et al* (1963) to the overlap between the wavefunctions for the orbitals.

A summary of atomic calculations for Fe XVI is given in Badnell and Moores (1994). The early DW work by Flower and Nussbaumer (1975) (n=3 only), Blaha and Davis (1978) and Mann (1983) was superceded by Sampson *et al* (1990), who carried out relativistic distorted wave calculations in the Na-like ions. This comprehensive study covers all the ions with nuclear charge in the range $22 \leq Z \leq 92$ for six values of the scattered electron energy. We have compared our results with Sampson *et al* and find very good agreement (better than 10 %) for all transitions except 3s - 5s, where there is a difference of 25 % for low energies. This could possibly be due to the more approximate potential used by us for the bound and free orbitals. The results for this transition agree better for high energies, indicating that the difference is not due to the relativistic nature of Sampson *et al*'s calculations.

Tayal (1994) has recently published Close Coupling (CC) results for Fe XVI obtained using the R-matrix method (including the 10 lowest fine structure states from the configurations - 3s, 3p, 3d, 4s, 4p, 4d). Tayal found the agreement between his non-resonant collision strengths with Flower and Nussbaumer's (1975) and Mann's (1983) values to be remarkably good. Unfortunately, he did not refer to the work by Sampson *et al* (1990). The resonance contribution to the effective collision strengths for the optically forbidden transitions is greatest at low temperatures ($< 10^6 K$), even then it was found to be quite small ($10 - 15\%$). Our total collision strengths agree to within 10% with those given by Tayal. We conclude that the agreement for the electron collision data for Fe XVI by the different authors is excellent.

**Table 4.** Collision strengths

| Transition i j | Ω 26 Ryd | 50 Ryd | 100 Ryd | 200 Ryd |
|---|---|---|---|---|
| 4 5 | 0.131 | 0.0945 | 0.0755 | 0.0740 |
| 4 6 | 0.0150 | 0.0152 | 0.0159 | 0.0132 |
| 4 7 | 0.0254 | 0.0396 | 0.0629 | 0.0911 |
| 4 8 | 0.0202 | 0.0182 | 0.0208 | 0.0250 |
| 4 9 | 0.278 | 0.291 | 0.294 | 0.289 |
| 4 10 | 0.0373 | 0.0214 | 0.0163 | 0.0135 |
| 4 11 | 1.0104 | 1.458 | 2.049 | 2.610 |
| 4 12 | 0.0590 | 0.0291 | 0.0210 | 0.0314 |
| 4 13 | 0.00367 | 0.00270 | 0.00258 | 0.00258 |
| 4 14 | 0.00509 | 0.00525 | 0.00739 | 0.0102 |
| 4 15 | 0.00745 | 0.00421 | 0.00356 | 0.00391 |
| 4 16 | 0.0507 | 0.0520 | 0.0523 | 0.0518 |
| 4 17 | 0.0176 | 0.00746 | 0.00427 | 0.00366 |
| 4 18 | 0.161 | 0.230 | 0.316 | 0.398 |
| 4 19 | 0.0297 | 0.00996 | 0.00477 | 0.00509 |
| 5 6 | 0.0225 | 0.0230 | 0.0240 | 0.0201 |
| 5 7 | 0.0126 | 0.00877 | 0.00740 | 0.00666 |
| 5 8 | 0.0560 | 0.0777 | 0.117 | 0.164 |
| 5 9 | 0.0372 | 0.0214 | 0.0165 | 0.0136 |
| 5 10 | 0.438 | 0.449 | 0.452 | 0.442 |
| 5 11 | 0.136 | 0.136 | 0.170 | 0.221 |
| 5 12 | 1.474 | 2.104 | 2.948 | 3.757 |
| 5 13 | 0.00548 | 0.00403 | 0.00387 | 0.00389 |
| 5 14 | 0.00518 | 0.00254 | 0.00169 | 0.00156 |
| 5 15 | 0.0137 | 0.0118 | 0.0149 | 0.0198 |
| 5 16 | 0.0174 | 0.00741 | 0.00426 | 0.00366 |
| 5 17 | 0.0859 | 0.0229 | 0.0816 | 0.0806 |
| 5 18 | 0.0431 | 0.0271 | 0.0276 | 0.0339 |
| 5 19 | 0.242 | 0.333 | 0.453 | 0.572 |
| 6 7 | 5.341 | 7.000 | 8.284 | 8.500 |
| 6 8 | 10.680 | 13.995 | 16.576 | 17.010 |
| 6 9 | 0.594 | 0.548 | 0.529 | 0.409 |
| 6 10 | 0.891 | 0.822 | 0.793 | 0.614 |
| 6 11 | 0.0975 | 0.0935 | 0.0973 | 0.0869 |
| 6 12 | 0.130 | 0.125 | 0.130 | 0.116 |
| 6 13 | 0.292 | 0.352 | 0.370 | 0.374 |
| 6 14 | 0.0168 | 0.0463 | 0.0949 | 0.155 |
| 6 15 | 0.0344 | 0.0874 | 0.177 | 0.290 |
| 6 16 | 0.0354 | 0.0469 | 0.0448 | 0.0173 |
| 6 17 | 0.0531 | 0.0702 | 0.0670 | 0.0258 |
| 6 18 | 0.0540 | 0.0598 | 0.0563 | 0.0354 |
| 6 19 | 0.0720 | 0.0797 | 0.0750 | 0.0472 |

The averaged collision strength, $\Upsilon$ is defined as

$$\Upsilon_{ij} = \int_0^\infty \Omega_{ij} exp(\frac{-E_j}{kT}) d(E_j/kT) \quad (1)$$

where $\Omega_{ij}$ is the collision strength for the transition $i$ to $j$, $E_j$ is the electron energy relative to the final state $j$, $k$ is the Boltzmann constant and $T$ is the electron temperature of the plasma.

**Table 5.** Collision strengths

| Transition i j | Ω 26 Ryd | 50 ryd | 100 Ryd | 200 Ryd |
|---|---|---|---|---|
| 7 8 | 0.748 | 0.630 | 0.570 | 0.443 |
| 7 9 | 9.087 | 12.150 | 14.761 | 15.684 |
| 7 10 | 0.130 | 0.133 | 0.141 | 0.152 |
| 7 11 | 0.598 | 0.549 | 0.528 | 0.406 |
| 7 12 | 0.0549 | 0.0445 | 0.0447 | 0.0441 |
| 7 13 | 0.0429 | 0.113 | 0.203 | 0.309 |
| 7 14 | 0.311 | 0.374 | 0.391 | 0.392 |
| 7 15 | 0.0484 | 0.0535 | 0.0483 | 0.0215 |
| 7 16 | 0.0419 | 0.155 | 0.322 | 0.508 |
| 7 17 | 0.0319 | 0.0299 | 0.0272 | 0.0169 |
| 7 18 | 0.171 | 0.247 | 0.250 | 0.130 |
| 7 19 | 0.0344 | 0.0270 | 0.0275 | 0.0214 |
| 8 9 | 1.973 | 2.590 | 3.123 | 3.321 |
| 8 10 | 16.452 | 21.980 | 26.701 | 28.386 |
| 8 11 | 0.241 | 0.213 | 0.207 | 0.171 |
| 8 12 | 1.0620 | 0.970 | 0.933 | 0.722 |
| 8 13 | 0.0843 | 0.240 | 0.438 | 0.674 |
| 8 14 | 0.0472 | 0.0555 | 0.0515 | 0.0232 |
| 8 15 | 0.700 | 0.836 | 0.865 | 0.839 |
| 8 16 | 0.0480 | 0.0715 | 0.105 | 0.133 |
| 8 17 | 0.109 | 0.331 | 0.652 | 1.00744 |
| 8 18 | 0.0938 | 0.108 | 0.110 | 0.0667 |
| 8 19 | 0.321 | 0.452 | 0.460 | 0.246 |
| 9 10 | 0.421 | 0.342 | 0.312 | 0.255 |
| 9 11 | 14.474 | 19.295 | 21.325 | 19.962 |
| 9 12 | 0.102 | 0.0700 | 0.0705 | 0.102 |
| 9 13 | 0.0600 | 0.0628 | 0.0584 | 0.0289 |
| 9 14 | 0.0844 | 0.217 | 0.377 | 0.564 |
| 9 15 | 0.0594 | 0.0769 | 0.103 | 0.125 |
| 9 16 | 0.792 | 0.921 | 0.935 | 0.898 |
| 9 17 | 0.0650 | 0.0471 | 0.0419 | 0.0228 |
| 9 18 | 0.878 | 1.980 | 3.199 | 4.413 |
| 9 19 | 0.0839 | 0.0495 | 0.0527 | 0.0491 |
| 10 11 | 1.142 | 1.453 | 1.598 | 1.533 |
| 10 12 | 20.717 | 27.588 | 30.490 | 28.558 |
| 10 13 | 0.0900 | 0.0948 | 0.0884 | 0.0438 |
| 10 14 | 0.0352 | 0.0295 | 0.0271 | 0.0158 |
| 10 15 | 0.182 | 0.406 | 0.678 | 0.991 |
| 10 16 | 0.0648 | 0.0475 | 0.0424 | 0.0231 |
| 10 17 | 1.230 | 1.416 | 1.434 | 1.368 |
| 10 18 | 0.153 | 0.196 | 0.287 | 0.371 |
| 10 19 | 1.298 | 2.869 | 4.624 | 6.370 |

**Table 6.** Collision strengths

| Transition i j | Ω 26 Ryd | 50 Ryd | 100 Ryd | 200 Ryd |
|---|---|---|---|---|
| 11 12 | 0.364 | 0.204 | 0.173 | 0.152 |
| 11 13 | 0.0200 | 0.0141 | 0.0130 | 0.00843 |
| 11 14 | 0.0359 | 0.0315 | 0.0287 | 0.0166 |
| 11 15 | 0.0338 | 0.0192 | 0.0170 | 0.0110 |
| 11 16 | 0.0965 | 0.118 | 0.171 | 0.235 |
| 11 17 | 0.0559 | 0.0245 | 0.0245 | 0.0251 |
| 11 18 | 1.130 | 1.210 | 1.207 | 1.155 |
| 11 19 | 0.124 | 0.0383 | 0.0291 | 0.0190 |
| 12 13 | 0.0267 | 0.0188 | 0.0173 | 0.0113 |
| 12 14 | 0.0180 | 0.00807 | 0.00702 | 0.00496 |
| 12 15 | 0.0752 | 0.0594 | 0.0535 | 0.0318 |
| 12 16 | 0.0456 | 0.0151 | 0.0116 | 0.00798 |
| 12 17 | 0.158 | 0.175 | 0.248 | 0.337 |
| 12 18 | 0.124 | 0.0383 | 0.0292 | 0.0191 |
| 12 19 | 1.551 | 1.630 | 1.623 | 1.549 |
| 13 14 | 11.432 | 18.987 | 21.448 | 20.418 |
| 13 15 | 22.867 | 37.957 | 42.863 | 40.781 |
| 13 16 | 1.652 | 1.305 | 1.104 | 0.626 |
| 13 17 | 2.478 | 1.957 | 1.655 | 0.938 |
| 13 18 | 0.365 | 0.313 | 0.291 | 0.162 |
| 13 19 | 0.487 | 0.417 | 0.388 | 0.215 |
| 14 15 | 2.182 | 1.467 | 1.171 | 0.668 |
| 14 16 | 20.546 | 35.251 | 41.753 | 40.972 |
| 14 15 | 2.182 | 1.467 | 1.171 | 0.668 |
| 14 16 | 20.546 | 35.251 | 41.753 | 40.972 |
| 14 17 | 0.366 | 0.351 | 0.328 | 0.217 |
| 14 18 | 2.215 | 1.734 | 1.450 | 0.798 |
| 14 19 | 0.176 | 0.155 | 0.143 | 0.0878 |
| 15 16 | 4.547 | 7.467 | 8.737 | 8.444 |
| 15 17 | 37.266 | 63.698 | 75.349 | 73.813 |
| 15 18 | 0.859 | 0.692 | 0.595 | 0.339 |
| 15 19 | 3.922 | 3.073 | 2.575 | 1.423 |
| 16 17 | 1.245 | 0.861 | 0.704 | 0.415 |
| 16 18 | 40.149 | 68.760 | 68.812 | 62.165 |
| 16 19 | 0.255 | 0.220 | 0.264 | 0.180 |
| 17 18 | 3.140 | 5.147 | 5.196 | 4.630 |
| 17 19 | 57.455 | 98.301 | 98.378 | 88.829 |
| 18 19 | 0.980 | 0.534 | 0.447 | 0.291 |

The electron collision rate is then given by the well known formula

$$q_{ij} = 8.63x10^6 T^{0.5} exp(-E_{ij}/kT)\Upsilon_{ij}/\omega_i \quad (2)$$

Burgess and Tully (1992) have developed a graphical procedure to fit the collision strengths and to obtain upsilon ($\Upsilon$). This method is discussed in Burgess *et al* (1988) and Lang *et al* (1990). We shall not repeat the details of the method here. In Fig. 3 we use this technique to plot the reduced $\Omega s$ for the 3s - 4s, 4p, 4d and 4f transitions. The reduced energies are such that 0 corresponds to threshold and 1 corresponds to infinite energy. The parameter C is used to scale the $\Omega s$ and the Energies. Our collision strengths behave well and tend smoothly to the high energy limit. The high energy limit for the 3s - 4p transition is obtained from the oscillator strength. For the 3s - 4d transition, a high energy value of 0.123 was clculated by Tully and Petrini (1991, private communication) using our target orbitals and the Coulomb Born approximation. This is slightly higher than the extrapolated value for our collision strengths. We also plotted the results of Sampson *et al* using this technique and again found a very consistent behaviour with energy and very close agreement with our results.

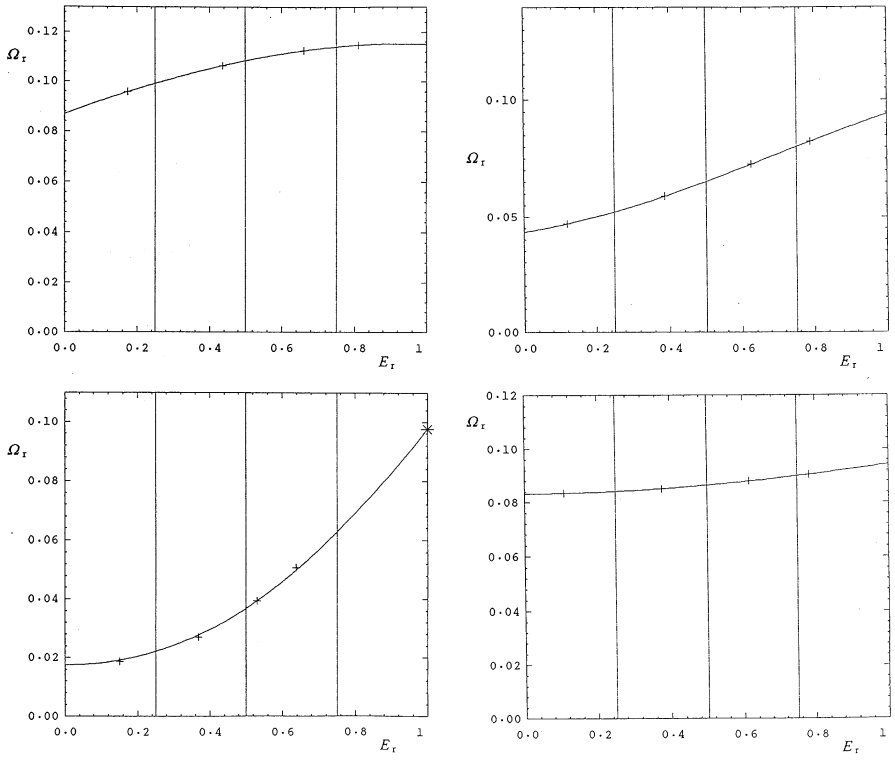

**Fig. 3.** Reduced collision strengths (after Burgess and Tully, 1992): top lhs 3s-4s, bottom hs 3s-4p, top rhs 3s-4d, bottom rhs 3s-4f, (scaling parameter is 2.5 for all plots)

## 4. Theoretical intensities

The statistical equilibrium equations for Fe XVI have been solved for the 19 lowest energy levels. The population of the ion for solar electron densities is almost entirely in the ground configuration and the theoretical intensity ratios are independent of electron density. The maximum abundance of Fe XVI is given as 2 x $10^6$ K (Arnaud and Rothenflug, 1985) or 2.5 x $10^6$ K (Arnaud and Raymond, 1992). There is a great deal of controversy concerning the precise values of the ionisation ratios for iron ions and indeed other elements. This will only be resolved by the availability of more accurate di-electronic recombination rates. The theoretical intensity ratios for the UV and the X-ray lines from Fe XVI have a temperature dependence due to the different variation of the collision strengths with energy.

**Table 7.** Theoretical intensites of the UV lines relative to I(335.40Å)

| $\lambda$(Å) | Transition | | $I^*/I$ at $2\text{x}10^6$ | $T_e$(K) $5\text{x}10^6$ | SERTS |
|---|---|---|---|---|---|
| 335.40 | 3s $^2S_{0.5}$ | 3p $^2P_{1.5}$ | 1.0 | 1.0 | 1.0 |
| 360.75 | 3s $^2S_{0.5}$ | 3p $^2P_{0.5}$ | 0.506 | 0.503 | 0.446 |
| 251.07 | 3p $^2P_{0.5}$ | 3d $^2D_{1.5}$ | 0.031 | 0.035 | 0.032 |
| 265.02 | 3p $^2P_{1.5}$ | 3d $^2D_{1.5}$ | 0.0053 | 0.0059 | 0.0020 |
| 262.98 | 3p $^2P_{1.5}$ | 3d $^2D_{2.5}$ | 0.054 | 0.061 | 0.049 |

## 5. Solar observations

### *5.1. UV lines*

The Fe XVI UV lines, corresponding to transitions within the n=3 configurations, fall between 250 - 370 Å. The Fe XVI UV lines were observed by both the HCO S0555 (300 - 1400 Å) (Vernazza and Reeves, 1978) and NRL S082A (171 - 630 Å) (Dere, 1978) instruments on Skylab. The sensitivity of the S0555 instrument fell rapidly towards the shorter wavelengths and the calibration was uncertain. Keenan *et al* (1994) have studied the Fe XVI UV lines in the NRL S082A observations, using the calculations of Tayal (1994). They found generally good agreement between the observed and theoretical values but were concerned about the saturation of the 335.40Åline on the photographic film for some of the spectra. The Fe XVI UV lines are clearly seen in the SERTS rocket spectra (230 - 400 Å) obtained by Neupert *et al* (1992). An atlas of intensities for an active region spectrum has been published by Thomas and Neupert (1994). In Table 7 we give a comparison of the observed (SERTS) and theoretical intensity ratios for the UV lines. We note the good agreement except for the weakest line at 265.02Å. All intensities in Table 7 and following tables are in units photons $\text{cm}^{-2}$ $\text{s}^{-1}$ $\text{arcsec}^{-2}$ (including those used to determine intensity ratios). The Fe XVI UV spectral lines are being studied with the Coronal Diagnostic Spectrometer (Harrison and Sawyer, 1992) on the Solar Heliospheric Observatory.

### *5.2. X-ray lines*

The X-ray lines between the n=3 and n=4, n=5 theoretical wavelengths are given in Table 8. Very few solar spectra have been recorded in this wavelength region. It is a very difficult region

**Table 8.** Theoretical relative intensities of the X-ray lines relative to I(50.57Å)

| λ(Å) | Transition | | $I^*/I$ at $T_e(10^6K)$ | | | |
|---|---|---|---|---|---|---|
| | | | 2 | 5 | 10 | 15 |
| 50.37 | 3s $^2S_{0.5}$ | 4p $^2P_{1.5}$ | 1.93 | 1.91 | 1.89 | 1.89 |
| 50.57 | 3s $^2S_{0.5}$ | 4p $^2P_{0.5}$ | 1.0 | 1.0 | 1.0 | 1.0 |
| 54.13 | 3p $^2P_{0.5}$ | 4d $^2D_{1.5}$ | 2.03 | 1.60 | 1.38 | 1.18 |
| 54.70 | 3p $^2P_{1.5}$ | 4d $^2D_{2.5}$ | 3.68 | 2.90 | 2.51 | 2.14 |
| 54.74 | 3p $^2P_{1.5}$ | 4d $^2D_{1.5}$ | 0.41 | 0.33 | 0.28 | 0.24 |
| 62.90 | 3p $^2P_{0.5}$ | 4s $^2S_{0.5}$ | 4.37 | 2.87 | 2.27 | 1.88 |
| 63.72 | 3p $^2P_{1.5}$ | 4s $^2S_{0.5}$ | 9.14 | 6.00 | 4.75 | 3.93 |
| 66.34 | 3d $^2D_{1.5}$ | 4f $^2F_{2.5}$ | 3.75 | 2.67 | 2.14 | 1.75 |
| 66.47 | 3d $^2D_{2.5}$ | 4f $^2F_{3.5}$ | 5.32 | 3.80 | 3.05 | 2.50 |
| 36.75 | 3s $^2S_{0.5}$ | 5p $^2P_{1.5}$ | 0.21 | 0.25 | 0.27 | 0.28 |
| 36.80 | 3s $^2S_{0.5}$ | 5p $^2P_{0.5}$ | 0.10 | 0.13 | 0.14 | 0.14 |
| 39.83 | 3p $^2P_{0.5}$ | 5d $^2D_{1.5}$ | 0.30 | 0.30 | 0.27 | 0.23 |
| 40.15 | 3p $^2P_{1.5}$ | 5d $^2D_{2.5}$ | 0.54 | 0.55 | 0.49 | 0.43 |
| 40.16 | 3p $^2P_{1.5}$ | 5d $^2D_{1.5}$ | 0.06 | 0.06 | 0.06 | 0.05 |
| 41.93 | 3p $^2P_{0.5}$ | 5s $^2S_{0.5}$ | 0.24 | 0.23 | 0.20 | 0.18 |
| 42.93 | 3p $^2P_{1.5}$ | 5s $^2S_{0.5}$ | 0.53 | 0.50 | 0.45 | 0.39 |
| 46.71 | 3d $^2D_{1.5}$ | 5f $^2F_{2.5}$ | 0.32 | 0.29 | 0.25 | 0.21 |
| 46.78 | 3d $^2D_{2.5}$ | 5f $^2F_{3.5}$ | 0.47 | 0.42 | 0.36 | 0.30 |

**Table 9.** XSST intensities of the Fe XVI X-ray lines

| λ(Å) | Transition | | i - j | 1982 | | 1985 |
|---|---|---|---|---|---|---|
| | | | | $I^*$ | $I^*/I$ | $I^*$ |
| 50.35 | 3s $^2S_{0.5}$ | 4p $^2P_{1.5}$ | 1- 8 | 204 | 1.98 | - |
| 50.55 | 3s $^2S_{0.5}$ | 4p $^2P_{0.5}$ | 1- 7 | 103 | 1.0 | - |
| 54.14 | 3p $^2P_{0.5}$ | 4d $^2D_{1.5}$ | 2- 9 | 167 | 1.62 | 17 |
| 54.73 | 3p $^2P_{1.5}$ | 4d $^2D_{2.5}$ | 3-10 | 238 | 2.31 | 38 |
| 54.73 | 3p $^2P_{1.5}$ | 4d $^2D_{1.5}$ | 3- 9 | 38 | 0.36 | 9 |
| 62.88 | 3p $^2P_{0.5}$ | 4s $^2S_{0.5}$ | 2- 6 | 216 | 2.09 | 25 |
| 63.72 | 3p $^2P_{1.5}$ | 4s $^2S_{0.5}$ | 3- 6 | 389 | 3.78 | 52 |
| 66.26 | 3d $^2D_{1.5}$ | 4f $^2F_{2.5}$ | 4-11 | 246 | 2.38 | 27 |
| 66.37 | 3d $^2D_{2.5}$ | 4f $^2F_{3.5}$ | 5-12 | 312 | 3.03 | 60 |

to observe because of low fluxes. Only the strongest lines were recorded in the grazing incidence photographic spectra obtained by rocket flights (Freeman and Jones, 1970). However, spectra in the 10 - 100 Å wavelength region have been obtained for a solar flare with the XSST instrument (Acton *et al*, 1985) in 1982.

Density diagnostics for these spectra were discussed in Brown *et al* (1986). Here we discuss only the Fe XVI line intensities. One major problem with this dataset is that the a partial failure in the mechanism to move the film resulted in two exposures being supperimposed on the same plate. A careful analysis of the plate is therefore required to separate the two spectra. However, the Fe XVI lines between 50 - 70 Å are a very strong feature of the spectra, as can be seen in Fig. 4.

The first exposure (45s) is to the right of the second exposure (145s). The first exposure spectral lines are slightly curved due to the distortion of the photographic plate. The summed densitometer scans in Fig. 4 are optimised for the second exposure. These are used to obtain the intensity values given in Table 3 of Acton *et al*. The calibration of the spectra as a function of wavelength and photographic intensity is also given in that paper. This has been carefully checked. Following a comprehensive study of UV photographic emulsions, the intensities were adjusted somewhat (by about 30% for the longest wavelengths $>$ 100Å). This only affected the Fe XVI lines very slightly. It is estimated that the relative intensities of the Fe XVI lines is accurate to about 20%. Another summed densitometer scan, optimised for the first exposure (Brown, 1985, unpublished) gives intensity ratios for the Fe XVI lines which agree very well with the second exposure.

The observed intensity ratios given in Fig. 4 are consistent with a temperature for emission of above 5 x $10^6$ K. This is significantly higher than the temperature for peak abundance of Fe XVI in ionisation equilibrium (2 - 2.5 x $10^6 K$, Arnaud and Rothenflug, 1985 or Arnaud and Raymond, 1992). The ionisation ratio is down by an order of magnitude on its peak value. However, these XSST spectra were taken 2 mins after the soft X-ray maximum of a solar flare. The temperature of the soft X-ray loops in solar flares is typically around $10^7$ K from observations by instruments such as those on SMM. The density is also usually significantly enhanced over its active region value. The electron density measured for this flare by Brown *et al* (1986) was 3 x $10^{10}$ cm$^{-3}$.

There seems to be little doubt about the high accuracy of both the atomic data and these XSST observations, so we must conclude that the FeXVI lines are being emitted at a temperature significantly in excess of the temperature for peak abundance.

The XSST instrument was flown again in 1985 and a non-flaring active region was observed. Results are given in Brunner *et al* (1988) and Brown *et al* (1988). The Fe XVI lines are much weaker than the 1982 spectra. Intensity values are given in Table 9, but the estimated errors are much greater. However, it is very interesting to note that the lines at 50.35 and 50.56 Å are not discernible above the noise level, whereas the line at 54.72 Å is quite strong. This is consistent with a much lower temperature of formation (2 x $10^6$ K or less) than for the 1982 spectra.

These Fe XVI spectral line ratios offer an ideal method of determining the electron temperature for active regions and flares. With good spectral resolution, they could also be used for stellar diagnostics.

## 6. Synthetic spectra

The X-ray and UV solar spectrum has been simulated by several authors using purely theoretical approximations (Kato, 1976, Mewe, 1972, Mewe *et al* 1981, 1985, Landini and Monsignori-Fossi, 1972, 1990, 1991) and semi-empirical methods (Doschek and Cowan, 1984). A comparison and critique of different plasma emission codes was published by Mason (1996). The approximation which is commonly used to estimate the intensity for the solar lines is based on the $\bar{g}$ formula (Van Regemorter, 1962).

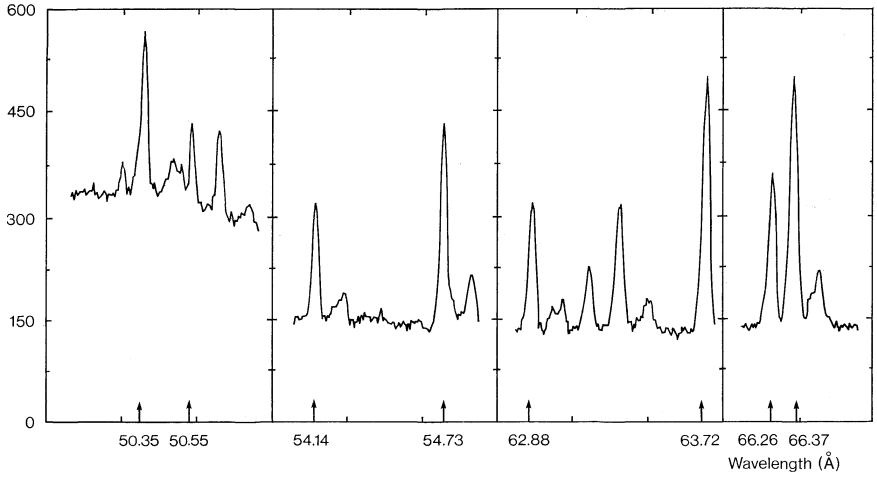


**Fig. 4.** XSST Observations of the Fe XVI X-ray lines

The averaged collision strength $\Upsilon$, which Mewe calls $\bar{\Omega}$ is related to $\bar{g}$ by

$$\Upsilon_{ij} = \frac{8\pi}{\sqrt{3}} \frac{\omega_i f_{ij}}{E_{ij}} \bar{g} \quad (3)$$

where $\omega_i f_{ij}$ is the radiative oscillator strength and $E_{ij}$ is the energy difference between levels $i$ and $j$.

It should be emphasised that the $\bar{g}$ formulation was developed for dipole transitions. Mewe (1972) extended its use to forbidden transitions. He uses an expression of the form

$$\bar{g} = A + (By - Cy^2 + Dy^3 + E)e^y E_1(y) + (C + D)y - Dy^2 \quad (4)$$

for both allowed and forbidden transitions. The parameters A,B,C,D and E are derived by fitting to available electron excitation rates. The parameter y is $E_{ij}/kT$, and $E_1(y)$ is a standard exponential integral.

Our $\Upsilon$s can be directly compared to the values obtained using Mewe's formulation. Such a comparison shows immediately that there is a major problem with Mewe's values for these X-ray lines. The formulation which he used is not appropriate for non-dipole transitions. For forbidden transitions, eqation (3) has no meaning, since the oscillator strength $\omega_i f_{ij}$ is not defined. Mewe suggested using the $f_{ij}$ of the nearest allowed transition. This was done by Kato, Mewe *et al* and Landini and Monsignori-Fossi. Doschek and Cowan (1984) produced a semi-empirical composite spectra from 10 to 200 Å. Their intensities were based on observed solar values. For the FeXVI lines between 50 and 70 Å, they used the spectra of Freeman and Jones (1970). Their intensity ratios are not in very good agreement with the XSST spectra. Mewe *et al* (1985) re-normalised the oscillator strengths ($f_{ij}$) used for FeXVI lines, with a fixed $\bar{g}$, based on the semi-empirical spectrum of Doschek and Cowan. Their value for the parameter A in equation (2) is 0.15, and B=C=D=E=0 except for the 50.40 Å line (3s - 4p) where E=0.276. This corresponds to a $\bar{g}$ of 0.15 for all the lines except 50.40 Å where $\bar{g}$ ranges from 0.15 at low temperatures to 0.7 at high temperatures. In contrast, the $\bar{g}$ for the 3s- 4p transition derived from our calculations ranges from 0.02 to 0.08. Landini and Monsignori-Fossi (1991) used the $f_{ij}$ corresponding to the spectral line observed. This does not correspond to the excitation transition. For example, consider the two Fe XVI lines at around 66Å. These correspond to to the transition $3d$ - $4f$. Mewe and Gronenschild (1981) used the $f_{ij}$ for the transition $3s$ - $4p$, whereas Landini and Monsignori-Fossi (1991) use the $f_{ij}$ for $3d$ - $4f$. Neither is in fact appropriate since, the lines arise from electron excitation between $3s$ - $4f$.

Sampson and Zhang (1992) studied the use of the Van Regemorter formula for collision strengths. Their abstract states *It is found to be a very poor approximation, especially for* $\Delta n \geq 1$ *excitation transitions from levels* $l < n - 1$*, and the recommendation is made that with recent advances in calculation procedures and available accurate atomic data, use of the Van Regemorter formula be discontinued*. We whole heartedly agree with their recommendation.

Since the Fe XVI X-ray lines have not been extensively studied with solar spectra, it is perhaps not so surprising that such major inconsistencies went unnoticed until recently (Brickhouse *et al*, 1995a). However these plasma emission codes have also been used to analyse astrophysical data, for example EXOSAT observations of stellar coronae ( Schrijver *et al* 1989, Lemen *et al* 1989), ROSAT (Schmitt, 1992) and DXS Bragg Crystal Spectrometer (44 - 83Å, Sanders and Edgar, 1996). For such analyses, large inaccuracies in the sythetic spectra for FeXVI could lead to a mis-interpretion of the distribution of material as a function of temperature. The plasma emission codes are now being updated using accurate Fe XVI electron scattering rates (cf Brickhouse *et al*, 1995b, Monsignori Fossi and Landini, 1994, 1996, Kaastra and Mewe, 1995, private communication).

## 7. Conclusions

We have used a new program (NELMA) for calculating the high partial wave contribution to the electron collision strength. Our results are in very close agreement with other published calculations. Having verified the accuracy of the methods used for Fe XVI, we intend to extend the NELMA calculations to other ions, for example FeXV, including transitions $3s^2$ - $3s4s$,

$3s4p$, $3s4d$, $3s4f$, which also give rise to very strong spectral lines in the X-ray wavelength region (Bhatia *et al*, 1996).

Our theoretical intensity ratios for the Fe XVI X-ray spectral lines are consistent with the solar observations. For the solar flare spectrum, the temperature for emission of FeXVI seems to be well in excess of the temperature corresponding to its peak ion abundance. The strength of the electron collision rates 3s - 4s, 4d, 4f compared to 3s - 4p demonstrates that extreme caution should be taken when using some published synthetic spectra. This has important consequences for analyses of other astrophysical (besides solar) X-ray spectra. A new atomic data base (CHIANTI) and UV synthetic spectral code ($> 50$ Å) has been prepared by Dere *et al* (1996). The electron excitation data are fitted following the graphical assessment method of Burgess and Tully (1992). CHIANTI is scheduled for release in July 1996 and will be available by anonymous FTP.

*Acknowledgements.* We wish to thank the PPARC-GB, CNRS-France and CELV-France.

## References

Acton, L.W., Bruner,M.E., Brown, W.A., Fawcett, B.C., Schweizer, W. and Speer, R.J., 1985, ApJ, 291, 865.
Arnaud, M. and Raymond, J.C. 1992, ApJ, 398, 39.
Arnaud, M. and Rothenflug, R. 1985, A&AS, 60, 425.
Badnell, N.R. and Moores, D.L. 1994, Atomic Data Nucl. Data Tabl., 57, 329.
Bely, O., Tully, J.A. and VanRegemorter, H. 1963, Ann. Phys., 8, 303.
Bhatia, A.K. and Mason, H.E. 1981, A&A, 103, 324.
Bhatia, A.K. and Mason, H.E. 1983, A&AS, 52, 115.
Bhatia, A.K., Mason, H.E. and Blancard, C. 1996, Atomic Data Nucl. Data Tables, submitted.
Blaha,M. and Davis, J. 1978, J. Quant. Spect. Rad. Trans., 19, 227.
Brickhouse, N.S., Edgar, R., Kaastra, J., Kallman, T., Liedahl, D., Masai, K., Monsignori Fossi, B., Petre, R., Sanders, W., Savin, D.W., Stern, R. 1995a, legacy.
Brickhouse, N.S., Raymond, J.C. and Smith, B.W. 1995b, A&AS, in press.
Brown, W.A., Bruner, M.E. and Acton, L.W. 1988, J. de Physique, 49, C1-259.
Brown, W.A., Bruner, M.E., Acton, L.W. and Mason, H.E. 1986, ApJ, 301, 981.
Bruner, M.E., Haisch, B.M., Brown, W.A., Acton, L.W. and Underwood, J.H. 1988, J. de Physique, 49, C1-115.
Burgess, A., Mason, H.E. and Tully, J.A. 1988, J. de Physique, 49, C1-107.
Burgess, A., Mason, H.E. and Tully, J.A. 1989, A&A, 217, 31.
Burgess, A., Mason, H.E. and Tully, J.A. 1991, ApJ, 376, 803.
Burgess, A. and Shoerey, V.B. 1974, J. Phys. B, 7, 2403.
Burgess, A. and Tully, J.A. 1992, A&A, 254, 436.
Cornille, M., Dubau, J.A., Mason, H.E., Blancard, C. and Brown, W.A. 1993, UV and X-ray Spectroscopy of Laboratory and Astrophysical Plasmas, eds. E. Silver and S. Kahn (publ. CUP), pp 101.
Cornille, M., Dubau, J. ,Faucher, P. ,Bely-Dubau, F. and Blancard, C. 1994, A&AS, 105, 77
Dere, K.P. 1978, ApJ, 221, 1062.
Dere, K.P., Landi, E., Mason, H.E., Monsignori Fossi, B.C. and Young, P.R. 1996, A&A, submitted.
Doschek, G.A. and Cowan, R.D. 1984, ApJS, 56, 67.
Eissner, W. 1972, Phys. of Elect. and Atomic Coll., VII ICPEAC, Amsterdam, publ. N. Holland, p460.
Eissner, W., Jones, M. and Nussbaumer, H. 1974, Comp. Phys. Comm., 8, 270.
Eissner, W. and Seaton, M.J. 1972, J. Phys. B, 5, 2187.
Flower, D.R. and Nussbaumer, H. 1975, A&A, 42, 265.
Freeman, F.F. and Jones, B.B. 1970, Sol. Phys., 15, 288.
Harrison, R.A. and Sawyer, E.C. 1992, in Proc. of the First SOHO Workshop, ESA SP-348, p17.
Kato, T 1976, ApJS, 30, 397.
Keenan, F.P., Conlon, E.S., Foster, V.J., Tayal, S.S. and Widing, K.G. 1994, ApJ, 432, 809.
Lang, J. 1994, Atomic Data Nucl. Data Tabl., 57.
Lang, J., Mason, H.E. and McWhirter, R.W.P. 1990, Sol. Phys., 129, 31.
Landini,M and Monsignori Fossi, B.C. 1972, A&AS, 7, 291.
Landini,M and Monsignori Fossi, B.C. 1990, A&AS, 82, 229.
Landini,M and Monsignori Fossi, B.C. 1991, A&AS, 91, 183.
Lemaire, P., Wilhelm, K., Axford, W.I., Curdt, W., Gabriel, A.H., Grewing, M., Huber, M.C.E., Jordan, S.D., Kuehne, M., Marsch, E., Poland, A.I., Thomas, R.J., Timothy, G.J., Vial, J.-C. 1992, in Proc. of the First SOHO Workshop, ESA SP-348, p13.
Lemen, J.R., Mewe, R., Schrijver, C.J. and Fludra, A. 1989, ApJ, 341, 474.
Mann, J.B. 1983, Atomic Data Nucl. Data Tabl., 29, 407.
Mason, H.E. 1996, IAU Colloquium no. 152 - Astrophysics in the EUV, Berkeley, March 27-30, 1995, eds. S. Bowyer and R.F. Malina, publ. Kluwer Academic Press, p561.
Mason, H.E. and Monsignori Fossi, B.C. 1994, The Astron. Astrophys. Rev., 6, 123.
McWhirter, R.W.P. 1994, Atomic Data Nucl. Data Tab., 57, 39.
Mewe, R. 1972, Sol. Phys., 22, 459.
Mewe, R. and Gronenschild, E.H.B.M. 1981, A&AS, 45, 11.
Mewe, R., Gronenschild, E.H.B.M. and van den Oord, G.H.J. 1985, A&AS, 62, 197.
Monsignori Fossi, B.C. and Landini, M. 1994, Sol. Phys., 152, 81.
Monsignori Fossi, B.C. and Landini, M. 1996, IAU Colloquium no. 152 - Astrophysics in the EUV, Berkeley, March 27-30, 1995, eds. S. Bowyer and R.F. Malina, publ. Kluwer Academic Press, p543.
Neupert, W.M., Epstein, G.L., Thomas, R.J. and Thompson, W.T. 1992, Sol. Phys., 137, 87.
Reader, J. and Sugar, J. 1975, J. Phys. Chem. Ref. Data, 4, 353.
Sampson, D.H. and Zhang, H.L. 1992, Phys. Rev. A, 45, 1556.
Sampson, D.H., Zhang, H.L. and Fontes, C.J. 1990, At. Data Nucl. Data Tables, 44, 209.
Sanders, W. and Edgar, R.J. 1996, IAU Colloquium no. 152 - Astrophysics in the EUV, Berkeley, March 27-30, 1995, eds. S. Bowyer and R.F. Malina, publ. Kluwer Academic Press, p269 .
Saraph, H.E. 1970, Comp. Phys. Commun., 1, 232.
Saraph, H.E. 1972, Comp. Phys. Commun., 3, 256.
Saraph, H.E. 1978, Comp. Phys. Commun., 15, 247.
Schmitt, J.H.M.M. 1992, in Seventh Cambridge Workshop on Cool Stars, Stellar Systems and the Sun, ASP Conf. Ser., 26, p83.
Schrijver, C.J., Lemen, J.R. and Mewe, R. 1989, ApJ, 341, 484.
Tayal, S.S. 1994, ApJ, 426, 449.
Thomas, R.J. and Neupert, W.M. 1994, A&AS, 91, 461.
Van Regemorter, H. 1962, ApJ, 136, 906.
Vernazza, J.E. and Reeves, E.M. 1978, ApJS, 37, 485.

This article was processed by the author using Springer-Verlag LaTeX A&A style file *L-AA* version 3.